

Original citation:

Li, Shuo, Wan, Chaoying, Wu, Xiaoyu and Wang, Shifeng. (2016) Core-shell structured carbon nanoparticles derived from light pyrolysis of waste tires. *Polymer Degradation and Stability*, 129 . pp. 192-198.

Permanent WRAP URL:

<http://wrap.warwick.ac.uk/78940>

Copyright and reuse:

The Warwick Research Archive Portal (WRAP) makes this work by researchers of the University of Warwick available open access under the following conditions. Copyright © and all moral rights to the version of the paper presented here belong to the individual author(s) and/or other copyright owners. To the extent reasonable and practicable the material made available in WRAP has been checked for eligibility before being made available.

Copies of full items can be used for personal research or study, educational, or not-for-profit purposes without prior permission or charge. Provided that the authors, title and full bibliographic details are credited, a hyperlink and/or URL is given for the original metadata page and the content is not changed in any way.

Publisher's statement:

© 2016, Elsevier. Licensed under the Creative Commons Attribution-NonCommercial-NoDerivatives 4.0 International <http://creativecommons.org/licenses/by-nc-nd/4.0/>

A note on versions:

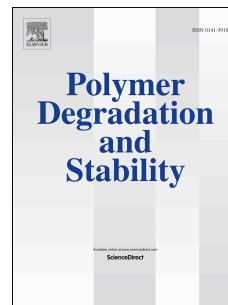
The version presented here may differ from the published version or, version of record, if you wish to cite this item you are advised to consult the publisher's version. Please see the 'permanent WRAP URL' above for details on accessing the published version and note that access may require a subscription.

For more information, please contact the WRAP Team at: wrap@warwick.ac.uk

Accepted Manuscript

Core-shell structured carbon nanoparticles derived from light pyrolysis of waste tires

Shuo Li, Chaoying Wan, Xiaoyu Wu, Shifeng Wang



PII: S0141-3910(16)30112-4

DOI: [10.1016/j.polymdegradstab.2016.04.013](https://doi.org/10.1016/j.polymdegradstab.2016.04.013)

Reference: PDST 7938

To appear in: *Polymer Degradation and Stability*

Received Date: 25 December 2015

Revised Date: 6 April 2016

Accepted Date: 22 April 2016

Please cite this article as: Li S, Wan C, Wu X, Wang S, Core-shell structured carbon nanoparticles derived from light pyrolysis of waste tires, *Polymer Degradation and Stability* (2016), doi: 10.1016/j.polymdegradstab.2016.04.013.

This is a PDF file of an unedited manuscript that has been accepted for publication. As a service to our customers we are providing this early version of the manuscript. The manuscript will undergo copyediting, typesetting, and review of the resulting proof before it is published in its final form. Please note that during the production process errors may be discovered which could affect the content, and all legal disclaimers that apply to the journal pertain.

1 **1. Introduction**

2 The ever growing transportation industry has driven the fast development of
3 modern society, but meanwhile induced serious pollution issues to the environment [1].
4 Waste tire disposal management is one of the major concerns, as about 1.4 billion unit
5 of tires are produced globally every year, and around 800 million tires are discarded
6 [2]. The present methods of disposal of waste tire rubbers include landfill, retreading
7 and pyrolysis [3,4]. Pyrolysis is an economical and environmental-friendly way to deal
8 with waste tire rubbers. It involves a process that heats tires over 400 °C in an oxygen
9 poor or free atmosphere to crack the organic components of rubber, and thus results in
10 pyrolytic carbon black (CB_p) as one of the main products [5-7]. As compared to
11 commercial carbon black (e.g., N330), CB_p generally has lower specific surface area
12 and higher ash content, which gives lower reinforcing efficiency to rubbers. These
13 limitations of CB_p hinder its industrialization and marketability [8-10].

14 To improve the performance of CB_p, different methods, such as developing high
15 efficient pyrolysis apparatuses, optimizing pyrolysis parameters and improving the
16 chemical activation of CB_p have been under developing[6,11-13]. For example,
17 microwave irradiation has the advantages of low heating cost, fast and direct heating of
18 any microwave absorbing material. The CB_p produced by microwave irradiation has a
19 small ash content in the range of 5.9-9.5 wt% [14]. Although this method reduces the
20 energy cost in the pyrolysis process, the properties of CB_p still cannot reach the level of
21 commercial carbon black. The properties of CB_p can be adjusted by either varying the
22 pyrolysis pressure [15] or atmosphere [16, 11]. The surface chemistry of CB_p obtained
23 at vacuum pressure is close to that of commercial carbon black due to its low ash
24 content. Pyrolytic atmosphere was also adopted to improve the specific surface area of
25 CB_p. With steam and CO₂, the specific surface area of CB_p reached 1000 m² g⁻¹ [11],
26 much larger than that of conventional CB_p, which is in the range of 54-87 m² g⁻¹ [15].
27 However, the complex procedures and expensive equipment restrict the industrial

1 application of this pyrolytic process.

2 It is challenging to separate carbon black from chemically crosslinked structures
3 of tire rubbers. Reactive extrusion is regarded as an efficient method to devulcanize the
4 crosslinked rubber, by applying high temperature with shear and chemical force
5 [16-19]. Tzoganakis et al. [20] used supercritical CO₂ to aid continuous
6 devulcanization of waste tire rubber. Shi et al. [21] combined the advantage of
7 twin-screw extrusion with an appropriate amount of desulfurizer to reclaim ground tire
8 rubber (GTR) into liquid rubber, which can be further used as a reactive softener for
9 tire rubber. The purpose of the aforementioned studies is to obtain high performance
10 devulcanized rubbers via reactive extrusion. Given the facily adjustable processing
11 parameters, such as compounding temperature and shearing force, reactive extrusion is
12 a potential technology to dissemble the three-dimensional crosslinked covalent
13 structure of rubbers, and subsequently recover carbon black nanoparticles.

14 Generally the reinforcement of rubbers with carbon black is largely due to the
15 formation of bound rubber, and the content of bound rubber can directly reflect the
16 interactions between rubber and carbon fillers. Bound rubber is formed by physical
17 and chemical interactions between rubber and carbon black during compounding, and
18 coated firmly as a shell layer on the surface of carbon black [22,23]. The particle size,
19 specific surface area and chemical functional groups of the carbon black determine
20 the formation of bound rubber. To enhance the bound rubber content, many techniques,
21 such as oxygen plasma treatment [23], graft modification and surface coating, have
22 been adopted to treat the surface of carbon black, in order to increase the content of
23 functional groups and reduce the particle size [24-27]. Wu et al. [23] used the
24 high-energy electron beam to irradiate carbon black to increase oxygen content and
25 reduce particle sizes. However, the aforementioned methods are mostly suitable for
26 original carbon black, and involve complex and costly processes. If the bound rubber
27 can be preserved in the process of pyrolysis, the carbon black with bound rubber

1 separated from recycled waste tires would be a new carbon material with some special
2 properties.

3 The aim of this study is to separate lightly pyrolytic carbon black (CB_{lp}) from
4 GTR by using a mild twin-extrusion process. A layer of bound rubber is preserved on
5 the surface of CB_{lp} after melt-extrusion and solvent extraction process, which is
6 detected by using FTIR and TGA. The structure, morphology and reinforcement
7 properties of CB_{lp} were characterized by using X-ray photoelectron spectroscopy
8 (XPS), X-ray diffraction (XRD), transmission electron microscope (TEM) and
9 dynamic light scattering (DLS), and also compared with commercial carbon black
10 (N330) and pyrolytic carbon black (CB_p).

11

12 **2. Experimental**

13 **2.1 Materials**

14 The GTR (600-700 μm) is shredded and ground at the ambient temperature from
15 whole used truck tire rubber. The GTR (Jiangsu Anqiang Rubber Co., Ltd) consists of
16 6.97 wt% soluble material, 40.25 wt% natural rubber, 14.64 wt% synthetic rubber,
17 30.44 wt% carbon black and 7.70 wt% inorganic filler. The content of acetone extract
18 is 16.3% and toluene extract is 36.4%, and the left is defined as light pyrolytic carbon
19 black. Commercial carbon black (N330) with primary particle size of 26-45 nm is
20 provided by Shanghai Cabot Carbon Black Co., Ltd. Pyrolytic carbon black (CB_p)
21 produced by high temperature (500-600 °C) pyrolysis, is supplied by Shandong Jintai
22 Co., Ltd.

23 Natural rubber (SCR WF) is supplied by Hainan Agribusiness Group Co., China.
24 The compounding ingredients, such as sulfur (S), zinc oxide (ZnO), and the
25 accelerator tetramethylthiuram disulfide and
26 N-Cyclohexyl-2-benzothiazolesulfenamide were industry grades.

1 2.2 Preparation

2 2.2.1 Preparation of CB_{ip}

3 CB_{ip} was prepared in two steps. Firstly, GTR was melt-compounded through a
4 reactive extrusion process by using an inter-meshed twin-screw extruder (ZE25A from
5 Berstorff GmbH, Germany). The screws have four heating/cooling zones with a L/D
6 ratio of 41 and a diameter of 25 mm. GTR was added through the hopper at a constant
7 throughput (5 kg h⁻¹). The screw rotation was set constant at 300 rpm and the
8 temperature was set at 300 °C for the four zones. The pyrolytic rubber compound was
9 completely dried in an oven at a temperature of 50 °C for 2 h.

10 Secondly, 2 g of the pyrolyzed rubber compound were extracted with acetone in a
11 Soxhlet apparatus for 48 h to remove polar and low molecular weight fraction such as
12 accelerator and plasticizer from the rubber. Subsequently, nonpolar components such as
13 soluble rubber were extracted with toluene for 72 h. The residual CB_{ip} was dried in a
14 vacuum oven at 50 °C for 1 h.

15

16 2.3 Characterization and measurement

17 2.3.1 Characterization

18 Carbon blacks samples N330, CB_{ip} and CB_p were characterized by using FTIR
19 Spectrum 100, Perkin Elmer, Inc. (USA), in the wavenumber range from 4000 to 350
20 cm⁻¹. A thermo-gravimetric analysis (TGA, Q5000IR, TA Instruments, USA) was used
21 to study the thermal degradation behavior of N330, CB_p and CB_{ip} in the temperature
22 range from room temperature to 700 °C at a heating rate of 10 °C min⁻¹. Particle size
23 analysis of N330, CB_{ip} and CB_p were performed with particle size analyzer ZS90
24 (Malvern Instruments Ltd., UK) at 25 °C. To prepare the suspension (0.02 g l⁻¹),
25 carbon black particles were dispersed into toluene under ultrasonication for 30 min.
26 The Brunauer-Emmett-Teller (BET) surface area of the three carbon blacks were
27 tested by using ASAP 2010 M+C (Micromeritics Instrument Corp., USA) with

1 nitrogen as the adsorbate at 100 °C. Transmission electron microscopy (TEM) was
2 conducted by using a JEM-2100 (JEOL Ltd., Japan). X-ray photoelectron spectroscopy
3 (XPS) analysis was carried out on an AXIS Ultra DLD (Shimadzu, Japan). X-ray
4 diffraction (XRD) analysis of the samples was performed with a D8 Advance (Bruker
5 Corporation, Germany). The patterns were scanned between 0 ° and 90 ° at a scanning
6 rate of 2 ° s⁻¹.

7 **2.3.2 Bound rubber extraction**

8 Natural rubber compounds with carbon black samples were prepared according
9 to the formulation: NR 100 phr (parts-per-hundred rubber), carbon black 30 phr, ZnO
10 5 phr, S 2 phr, stearic acid 1 phr, TMTD 0.5 phr, CZ 0.5 phr. The mixing was carried
11 out in a S(X)K-160A Two-Roll mill from Shanghai light industry machinery Co., Ltd
12 (China). The compounds were vulcanized for 330 s ($t_{c,90}$) in a hydraulic press
13 (LP-S-50, Labtech Thailand) at 143 °C and 10400 kPa into 1 mm thick sheets.

14 Total bound rubber contents of the rubber compounds of NR/N330, NR/CB_{ip} and
15 NR/CB_p compounds were determined by extracting the unbound rubber with toluene
16 at ambient temperature for 7 days and then dried at 50 °C for 24 h. The content of
17 bound rubber was calculated according to Eq.1,

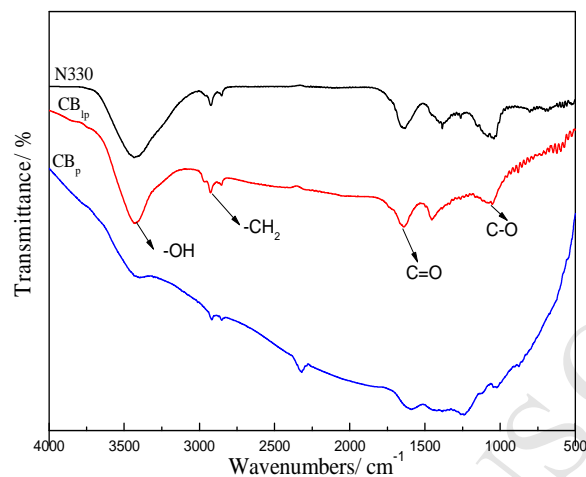
$$18 \quad R_b (\%) = (W_A - W_{CB}) / (W_B - W_{CB}) \cdot 100 \quad (1)$$

19 Where R_b is the contents of bound rubber, W_A is the weight of compounds after
20 extraction, W_{CB} is the weight of carbon black, W_B the weight of compounds before
21 extraction [28].

22 **2.3.3 Mechanical testing of NR/carbon black composites**

23 Tensile testing was conducted using universal mechanical tester (Instron 4465,
24 Instron Corp., USA) at room temperature. For each sample, six dumbbell shape
25 specimens of dimension of 75 x 4 x 1 mm³ were tested at 200 mm min⁻¹, and average
26 results were obtained for comparison.

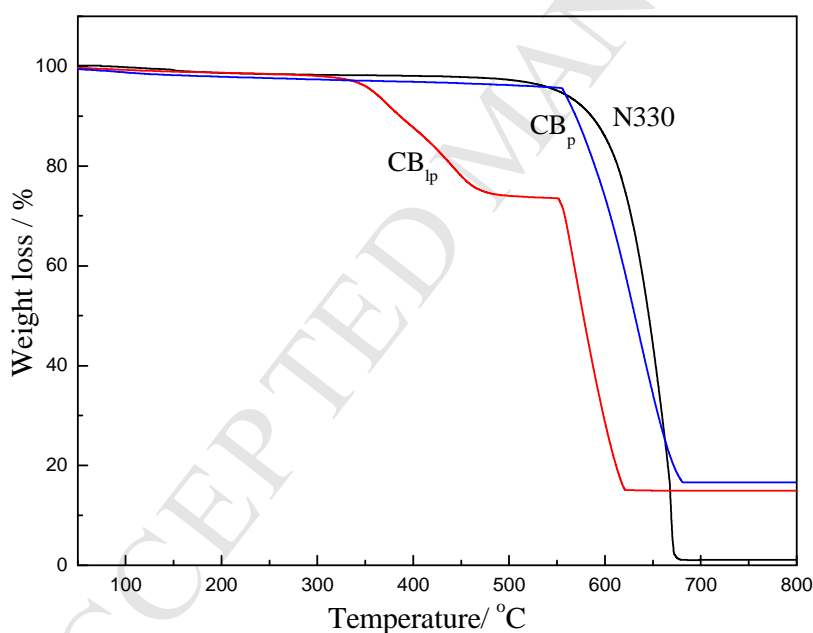
27

1 **3. Results and discussion**2 **3.1 Characterization of carbon blacks**3
4 Fig. 1. FTIR spectra of N330, CB_{1p} and CB_p

5 The derived CB_{1p} was characterized by FTIR and in comparison with commercial
6 N330 and CB_p. As shown in Fig. 1, the three spectra are baseline corrected and
7 normalized to the -CH₃ deformation vibration peak at 1375 cm⁻¹ [31]. CB_{1p} shows
8 similar absorption peaks as N330, but with weaker intensities for peaks at around 3435
9 and 1084 cm⁻¹, which are attributed to the stretching vibration of -OH and -C-O,
10 respectively [32]. This can be caused by the reactions of CB_{1p} with rubbers during the
11 compounding process, which consumes parts of the functional groups on the CB_{1p}
12 surface [22,33,34]. The peak around 2923 cm⁻¹ is attributed to the stretching vibration
13 of -CH₂ [35,36], it was observed on both surface of CB_{1p} and N330, indicating some
14 organic matter left on the surface of CB_{1p} and N330. The peak around 1632 cm⁻¹ is
15 attributed to the stretching vibration of -C=O [35,36]. Some free radicals can be
16 generated in the process of pyrolysis of GTR rubbers, and further react with -CH=CH
17 group of the carbon chains[37,38], the oxidization of the free radicals may form the
18 -C=O group on the surface of CB_{1p}. The characteristic peaks of -C=C and -C=O of CB_{1p}
19 overlap together, which enhances the intensity of -C=O of CB_{1p}. Moreover, the
20 intensities of functional groups of -OH, C-O, -CH₂, and -C=O of CB_{1p} are stronger than

1 those of CB_p . This may be due to the destruction of functional groups of CB_p is more
2 severe than CB_{ip} under the higher processing temperature (500 °C), or the deposit of
3 ash on the surface of CB_p [8].

4 Different pyrolytic processes of tire rubber will lead to different structures of
5 carbon black. To understand the composition of N330, CB_p and CB_{ip} the thermal
6 degradation behavior was examined by TGA. As shown in Fig. 2, CB_p and N330 have a
7 similar decomposition behavior when temperature is below 600 °C. N330 decomposes
8 completely at above 700 °C, while CB_p has about 16 wt% residues, which should be
9 ascribed to its ash constituent. CB_{ip} starts to degrade from 350 °C, followed with a
10 distinct weight loss of 18 wt% between 350 °C and 550 °C, which corresponds to the
11 decomposition of the bound rubber layer.



12

13

Fig. 2. TGA results of CB_p , CB_{ip} and N330

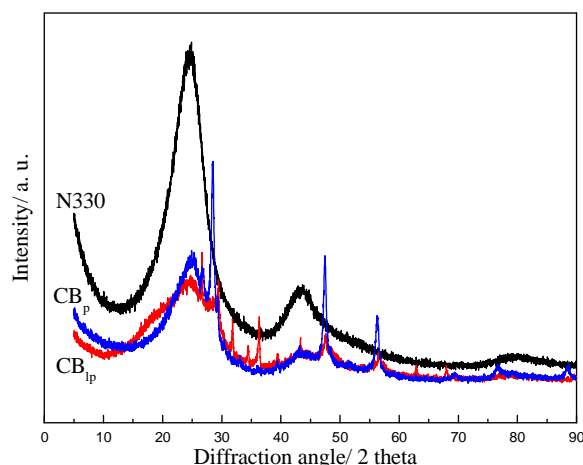
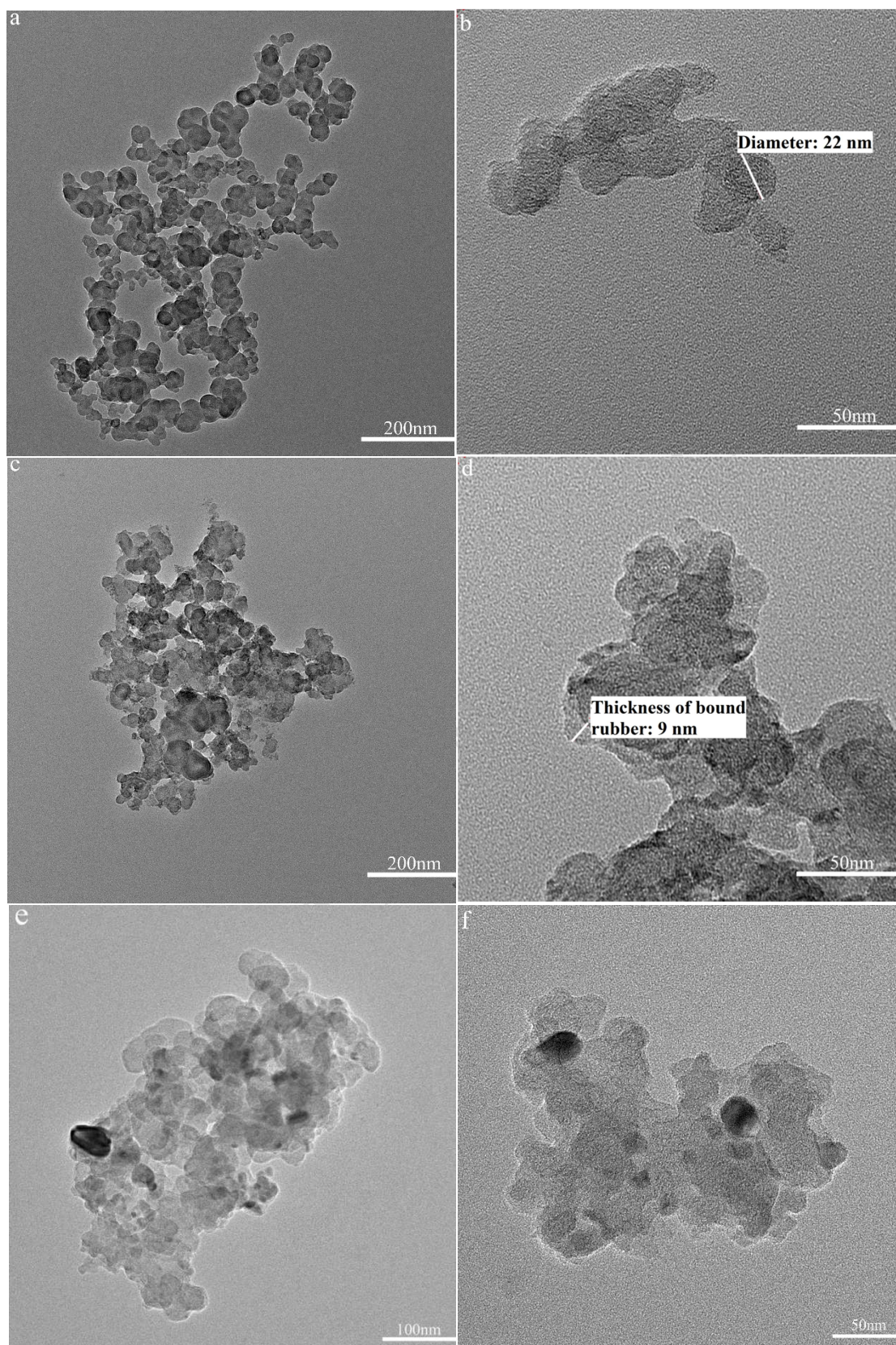


Fig. 3. X-ray diffraction patterns of N330, CB_{ip} and CB_p

As shown in Fig. 3, the three carbon black particles N330, CB_{ip} and CB_p show different diffraction patterns. The diffraction peak at 25.5 ° is attributed to the more crystalline/ordered phase characteristic of carbon black [39]. The peaks at 31.80 °, 34.40 °, 36.28 °, 47.58 °, 56.62 ° and 62.92 ° are corresponding to the ZnO [40,41], while 27.10 °, 28.20 °, 31.00 °, 39.20 °, 47.58 °, 51.80 °, 55.70 °, 56.62 ° and 57.80 ° are ascribable to the ZnS [40]. The broad bands at 34.40°, 36.28° and 62.92° reflect the characteristic peaks of ZnO which can only be observed in CB_{ip}, this indicates that most ZnO was transformed into ZnS in CB_p, while some ZnO is still exist in CB_{ip}.

As characterized by TEM, primary N330 particles are about 22 nm in diameter, and are aggregated together (Fig. 4ab). The aggregates of CB_{ip} and CB_p are filled or covered by bound rubber or ash (Fig. 4c-e). As shown in Fig. 4d, there is a layer of bound rubber with a thickness of about 7~12 nm on the surface of CB_{ip}, which can be well-preserved in the condition of light pyrolysis due to the strong interactions between the carbon black and rubber [23,42].



1

2

Fig. 4. TEM micrographs of (a-b)N330, (c-d)CB_{1p} and (e-f) CB_p

1 In comparison, the surface of CB_p is covered with a layer of ash, which is mainly
 2 derived from the deposition of inorganic filler during the pyrolysis of waste tire
 3 rubber at high temperature[8]. In this situation, the carbon black particles act as seed,
 4 to allow inorganic fillers to absorb and deposit onto its surface, which is shown as
 5 black dots in Fig.4 e-f [43,44]. The surface chemical structure of the different carbon
 6 black particles was further characterised by XPS, in order to elucidate the
 7 composition of the shell materials.

8 The elemental composition on the surface of N330, CB_{lp} and CB_p are presented in
 9 Table 1. The contents of elements C, N and S on the surface of CB_{lp} are higher than that
 10 of N330, while the contents of O is lower than N330, indicating an organic layer was
 11 attached on the surface of CB_{lp} , also in agreement with the result of FTIR (Fig.1). The
 12 bound rubber on the surface of CB_{lp} suppresses the expression of O element, while the
 13 presence of crosslink agent and accelerator in bound rubber provide the elements of S
 14 and N. In the high temperature pyrolysis of tire rubber, gases like H_2S and NH_3 are
 15 released [43,45], and left lower content of N and S on the surface of CB_p . In comparison,
 16 the light pyrolysis of tire rubber will give higher concentration of N and S on the
 17 surface of CB_{lp} .

18 Table 1 surface compositions of N330, CB_{lp} and CB_p tested by XPS

Carbon black	Surface composition /wt%			
	C	N	O	S
N330	88.38	0	11.46	0.16
CB_{lp}	91.22	1.27	5.43	2.09
CB_p	92.39	0.83	5.64	1.14

19 The curve fitting of C_{1s} photo peaks of XPS spectrum are shown in Fig.5 (a). The
 20 XPS spectrum of C_{1s} for N330, CB_{lp} and CB_p are fitted to four peaks: C-C or C-H (C_1 ,
 21 $BE=284.8$ eV), C-O (C_2 , $BE=285.5$ eV), C=O (C_3 , $BE=286.7$ eV), and COOH (C_4 ,
 22 $BE=289.0$ eV) [23,41,46]. The results of the curve-fitting of the C_{1s} spectrum are

1 summarized in Table 2.

2 Table 2 Area of the C_{1s} peaks of carbon black N330, CB_{ip} and CB_p

Compound	Area of C_{1s} peaks /at%			
	C_1 (C-H or C-C)	C_2 (C-O)	C_3 (C=O)	C_4 (COOH)
N330	45.99	28.67	12.85	12.49
CB_{ip}	69.37	17.90	5.29	7.44
CB_p	51.62	33.39	14.99	0

3

4 As shown in the Table 2, CB_{ip} has the highest content of C-C or C-H among the
5 three samples, indicating a rubber shell coated on the surface of CB_{ip} . The peak of
6 COOH is not observed in the spectrum of CB_p , which should be destroyed in the
7 process of pyrolysis at high temperature [41]. The existence of COOH functional
8 groups will make CB_{ip} more reactive than CB_p .

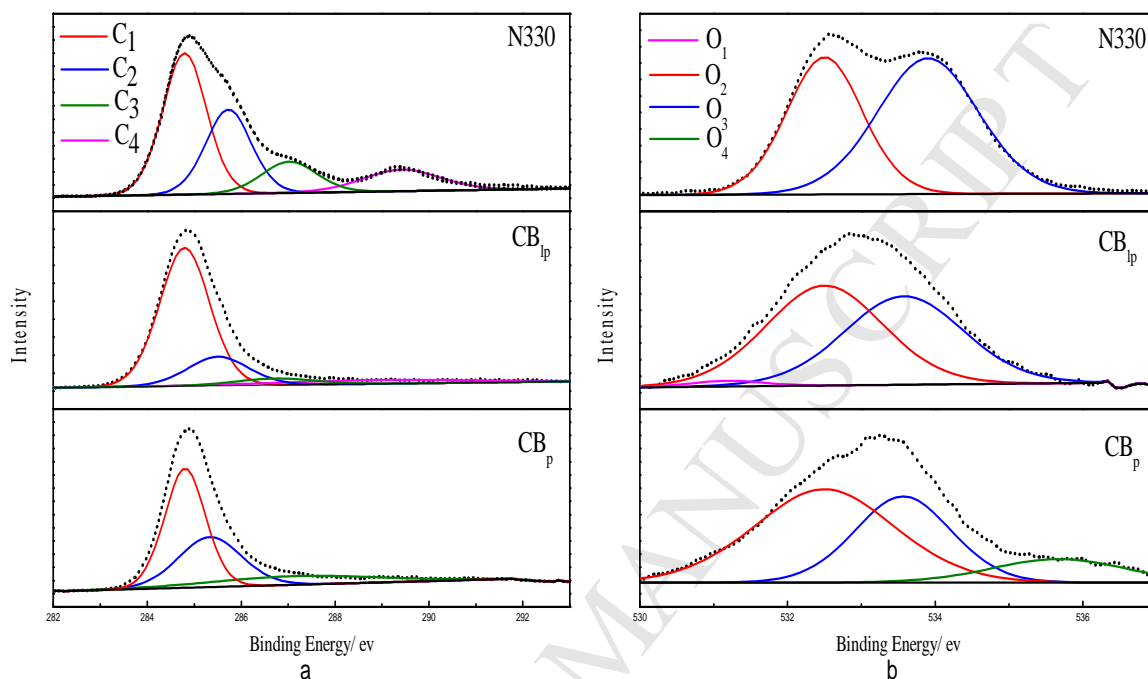
9 As shown in Fig. 5 (b) , the O_{1s} spectra are fitted to four peaks: a peak with a
10 binding energy of 531.0 eV (O_1) assigned to oxide oxygen, peaks at 532.5 eV(O_2),
11 533.5 eV(O_3) and 535.8 eV(O_4) are assigned to the C=O, C-O groups and a shake-up
12 peak, respectively [41]. The results of the curve-fitting of the O_{1s} spectra are shown in
13 Table 3.

14 Table 3 Area of the O_{1s} of carbon black N330, CB_{ip} and CB_p

Compound	Area of O_{1s} peaks /at%			
	O_1	O_2 (C=O)	O_3 (C-O)	O_4
N330	0	43.12	56.88	0
CB_{ip}	1.84	51.61	46.55	0
CB_p	0	53.27	33.87	12.86

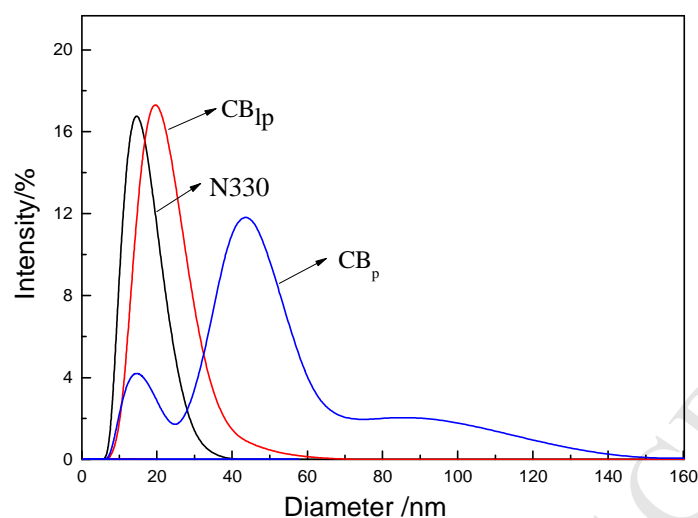
15 It is interesting to see that the oxide peak is only found in CB_{ip} , and absent in both
16 N330 and CB_p . The intensity of C=O in CB_p is the highest among the three samples
17 because of the oxidation of pyrolytic carbon. The ratio of C=O to C-O on the surface of

1 CB_{1p} is higher than N330. Moreover, the shake-up peak is not observed in the spectrum
 2 of N330 and CB_{1p}, showing that there is no free oxygen molecules existing in or close
 3 to the aromatic system on the surface of N330 and CB_{1p} [41]. This phenomenon also
 4 proves that the chemical structure of CB_{1p} is more similar to N330 rather than CB_p.



5
 6 Fig. 5. (a) C_{1s} XPS spectrum of carbon black N330, CB_{1p} and CB_p; and (b) O_{1s} XPS
 7 spectrum of carbon black N330, CB_{1p} and CB_p.

8 The average primary particle size of N330 is estimated to be 21 nm (also shown
 9 in TEM, Fig.4), and the smaller size results in higher specific surface area, as shown
 10 in the Table 4. The existence of bound rubber on the surface of CB_{1p} increases the
 11 particle size to about 29 nm. The particle size and Polydispersity Index (PDI) of CB_p
 12 is higher than that of N330 and CB_{1p} because some organic volatiles were released
 13 during the pyrolysis of GTR, and transformed into ash and absorbed on the surface of
 14 CB_p [43,45](Fig. 6). The Brunauer-Emmett-Teller (BET) surface area of CB_{1p} is
 15 lower than CB_p due to the coverage of the rubber on the surface(Table 4).



1

2

Fig. 6. Particle size distribution of N330, CB_{1p} and CB_p

3

Table 4 Particle size distribution and BET of N330, CB_{1p} and CB_p

Carbon black	Z-Average (r.nm)	PDI	BET surface area /m ² g ⁻¹
N330	21	0.247	64
CB _{1p}	29	0.290	16
CB _p	86	0.606	38

4

According to the analysis above, the separation process of carbon black (CB_{1p}) out of

5

lightly pyrolyzed GTR rubber is proposed and shown in Scheme 1. The chemical

6

network is firstly degraded and destroyed in the pyrolysis process of crosslinked

7

rubber. The interfacial interactions between rubber chains and carbon blacks could

8

induce a layer of bound rubber at the interface [29,30], and can be further reinforced

9

during vulcanization reactions. The highly crosslinked bound rubber layers are

10

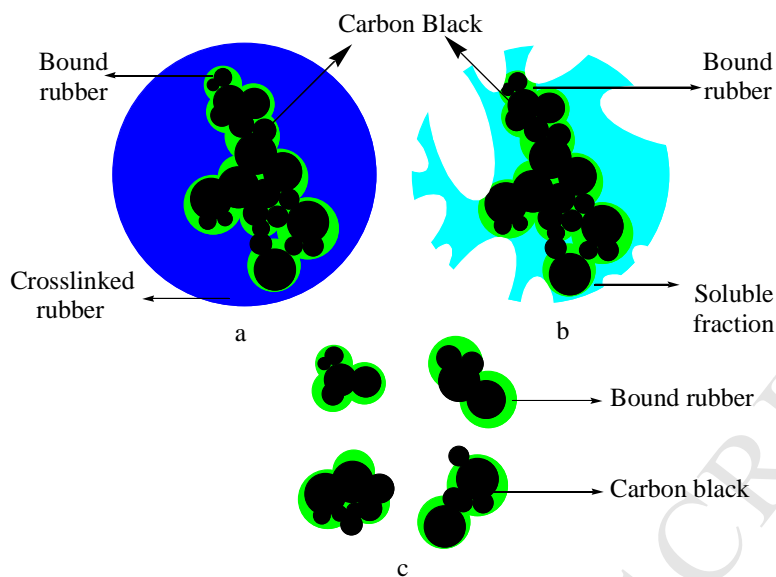
thermally stable that can stand the light pyrolysis (up to 300 °C) treatment, as well as

11

chemically robust during solvent extraction process, which are confirmed by the

12

characterisation results of FTIR, TGA, TEM and XPS.



1
2 Scheme 1. The separation process of carbon black and rubber in light pyrolysis (a, GTR;
3 b, lightly pyrolytic rubber; c, CB_{1p})

4 3.2 Mechanical properties

5 Natural rubber containing N330, CB_{1p} and CB_p are studied to evaluate the
6 reinforcement effects of the different carbon black particles. The stress-strain curves
7 of NR/N330, NR/CB_{1p} and NR/CB_p compounds are presented in Fig. 7. NR/CB_{1p}
8 compounds show higher content of bound rubber, tensile strength and elongation at
9 break than NR/N330 and NR/CB_p compounds (Table 5). The presence of bound
10 rubber layer on CB_{1p} surface helps the dispersion and interfacial interactions with
11 natural rubber, which critically affects the mechanical properties of the filled rubber
12 compounds [30].

13 Table 5 Mechanical properties of N330/NR, CB_{1p}/NR and CB_p/NR compounds

Carbon Black	Content of bound rubber /wt%	Elongation at break /%	Tensile Strength /MPa
N330/NR	49.8	275±5	6.1±0.2
CB _{1p} /NR	64.3	394±3	7.5±0.3
CB _p /NR	39.3	350±5	5.2±0.2

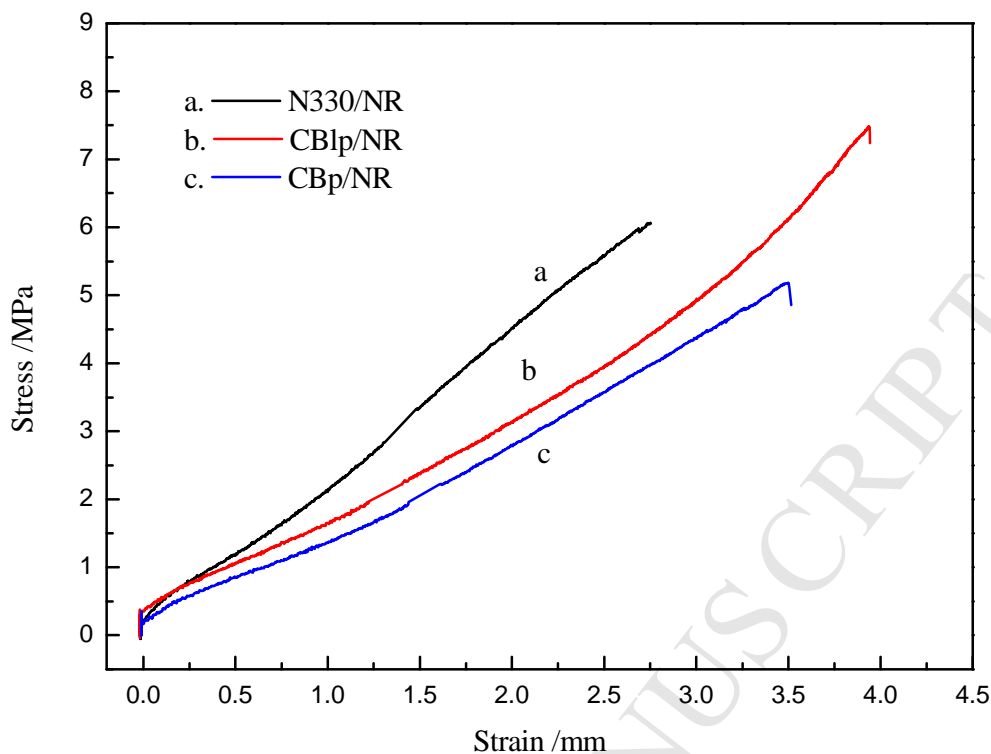


Fig. 7. Stress-strain curves of N330/NR, CB_{1p}/NR and CB_p/NR compounds

4. Conclusions

Core-shell structured CB_{1p} particles were derived from waste tire rubber by reactive melt-extrusion. The bound rubber layer on the surface of CB_{1p} was preserved during the light pyrolysis and toluene-extraction processes. The sulfur bond, filler and chemical additives in bound rubber have an influence on the chemical structure and morphological characteristics of CB_{1p}. The bound rubber increased the contents of N, S and functional group of -CH₂, while reduced the oxygenic functional groups on the surface of CB_{1p}. More functional groups and ZnO were preserved on the CB_{1p} surface than CB_p due to the mild pyrolysis process. As a consequence, the CB_{1p} showed higher reinforcement effect than CB_p due to the existence of bound rubber. The light pyrolysis is proven to be an environmental-friendly and efficient method for waste tire rubber disposal and a promising technique for producing core-shell structured carbon nanofillers.

1 **Acknowledgements:**

2 This research is supported by an International cooperation project (No.
3 2013DFR50550) and Natural Science Foundation of China (No. 51273110).

4 **References**

5 [1] Mark JE, Erman B, Roland CM. The Science and Technology of Rubber. 4th ed. Boston:
6 Academic Press. 2013: 697-764.

7 [2] Ramarad S, Khalid M, Ratnam C, Chuah AL, Rashmi W. Waste tire rubber in polymer blends: A
8 review on the evolution, properties and future. *Progress in Materials Science* 2015; 72;100-40.

9 [3] Duan P, Jin B, Xu Y, Wang F. Co-pyrolysis of microalgae and waste rubber tire in supercritical
10 ethanol. *Chemical Engineering Journal* 2015; 269;262-71.

11 [4] Undri A, Meini S, Rosi L, Frediani M, Frediani P. Microwave pyrolysis of polymeric materials:
12 Waste tires treatment and characterization of the value-added products. *Journal of Analytical and*
13 *Applied Pyrolysis* 2013; 103;149-58.

14 [5] Aguado J, Serrano DP, Escola JM. Fuels from waste plastics by thermal and catalytic processes:
15 A review. *Industrial and Engineering Chemistry Research* 2008; 47(21);7982-92.

16 [6] Choi GG, Jung SH, Oh SJ, Kim JS. Total utilization of waste tire rubber through pyrolysis to
17 obtain oils and CO₂ activation of pyrolysis char. *Fuel Processing Technology* 2014; 123;57-64.

18 [7] López G, Olazar M, Aguado R, Bilbao J. Continuous pyrolysis of waste tyres in a conical
19 spouted bed reactor. *Fuel* 2010; 89(8);1946-52.

20 [8] Williams PT. Pyrolysis of waste tyres: A review. *Waste Management* 2013; 33(8);1714-28.

21 [9] Chala A, Darmstadt H, Roy C. Acid-base method for the demineralization of pyrolytic carbon
22 black. *Fuel Processing Technology* 1996; 46(1);1-15.

23 [10] Ucar S, Karagoz S, Ozkan AR, Yanik J. Evaluation of two different scrap tires as hydrocarbon
24 source by pyrolysis. *Fuel* 2005; 84(14-15);1884-92.

25 [11] Saleh TA, Gupta VK. Processing methods, characteristics and adsorption behavior of tire
26 derived carbons: A review. *Advances in Colloid and Interface Science* 2014; 211;93-101.

27 [12] Mui ELK, Ko DCK, McKay G. Production of active carbons from waste tyres - A review.
28 *Carbon* 2004; 42(14);2789-805.

- 1 [13] Murillo R, Aylón E, Navarro MV, Callén MS, Aranda A, Mastral AM. The application of
2 thermal processes to valorise waste tyre. *Fuel Processing Technology* 2006; 87(2);143-7.
- 3 [14] Undri A, Sacchi B, Cantisani E, Toccafondi N, Rosi L, Frediani M, et al. Carbon from
4 microwave assisted pyrolysis of waste tires. *Journal of Analytical and Applied Pyrolysis* 2013;
5 104;396-404.
- 6 [15] Mikulova Z, Sedenkova I, Matejova L, Večeř M, Dombek V. Study of carbon black obtained by
7 pyrolysis of waste scrap tyres. *Journal of Thermal Analysis and Calorimetry* 2013; 111(2);1475-81.
- 8 [16] Kojima M, Ogawa K, Mizushima H, Tosaka M, Kohjiya S, Ikeda Y. Devulcanization of
9 sulfur-cured isoprene rubber in supercritical carbon dioxide. *Rubber chemistry and technology* 2003;
10 76(4);957-68.
- 11 [17] Mouri M, Sato N, Okamoto H, Matsushita M, Honda H, Nakashima K, et al. Continuous
12 Devulcanisation by Shear Flow Stage Reaction Control Technology for Rubber Recycling. Part 4. Study
13 of the Devulcanisation Process for EPDM. *POLYMER RECYCLING* 2000; 5(1);31-42.
- 14 [18] Fukumori K, Matsushita M, Okamoto H, Sato N, Takeuchi K, Suzuki Y. A New Material
15 Recycling Technology for Automobile Rubber Waste[R]. SAE Technical Paper, 2003.
- 16 [19] Gałol M, Boczkaj G, Haponiuk J, Formela K. Investigation of volatile low molecular weight
17 compounds formed during continuous reclaiming of ground tire rubber. *Polymer Degradation and*
18 *Stability* 2015; 119;113-20.
- 19 [20] Meysami M, Tzoganakis C. Continuous Rubber Devulcanization Using Supercritical Co₂:
20 Recycling Tire Rubber Crumb[C]. 8th World Congress of Chemical Engineering.
- 21 [21] Shi J, Zou H, Ding L, Li X, Jiang K, Chen T, et al. Continuous production of liquid reclaimed
22 rubber from ground tire rubber and its application as reactive polymeric plasticizer. *Polymer Degradation*
23 *and Stability* 2014; 99;166-75.
- 24 [22] Leblanc JL. Rubber-filler interactions and rheological properties in filled compounds. *Progress*
25 *in Polymer Science (Oxford)* 2002; 27(4);627-87.
- 26 [23] Wu Y, Wen S, Shen J, Jiang J, Hu S, Zhang L, et al. Improved dynamic properties of natural
27 rubber filled with irradiation-modified carbon black. *Radiation Physics and Chemistry* 2015; 111;91-7.
- 28 [24] Soares MCF, Viana MM, Schaefer ZL, Gangoli VS, Cheng Y, Caliman V, et al. Surface

1 modification of carbon black nanoparticles by dodecylamine: Thermal stability and phase transfer in
2 brine medium. *Carbon* 2014; 72:287-95.

3 [25] Guha A, Lu W, Zawodzinski Jr TA, Schiraldi DA. Surface-modified carbons as platinum
4 catalyst support for PEM fuel cells. *Carbon* 2007; 45(7):1506-17.

5 [26] Toupin M, Bélanger D. Thermal stability study of aryl modified carbon black by in situ
6 generated diazonium salt. *Journal of Physical Chemistry C* 2007; 111(14):5394-401.

7 [27] Zhang BB, Chen Y, Wang F, Hong RY. Surface modification of carbon black for the
8 reinforcement of polycarbonate/acrylonitrile-butadiene-styrene blends. *Applied Surface Science* 2015;
9 351:280-8.

10 [28] Choi S-S. Influence of storage time and temperature and silane coupling agent on bound rubber
11 formation in filled styrene-butadiene rubber compounds. *Polymer Testing* 2002; (21):201-8.

12 [29] Litvinov VM, Orza RA, Klüppel M, Van Duin M, Magusin PCMM. Rubber-filler interactions
13 and network structure in relation to stress-strain behavior of vulcanized, carbon black filled EPDM.
14 *Macromolecules* 2011; 44(12):4887-900.

15 [30] Choi S-S, Ko E. Novel test method to estimate bound rubber formation of silica-filled solution
16 styrene-butadiene rubber compounds. *Polymer Testing* 2014; 40:170-7.

17 [31] Forster AL, Pintus P, Messin GH, Riley MA, Petit S, Rossiter W, et al. Hydrolytic stability of
18 polybenzobisoxazole and polyterephthalamide body armor. *Polymer Degradation and Stability* 2011;
19 96(2):247-54.

20 [32] Liu H, Wen S, Wang J, Zhu Y. Preparation and characterization of carbon black - polystyrene
21 composite particles by high - speed homogenization assisted suspension polymerization. *Journal of*
22 *Applied Polymer Science* 2012; 123(6):3255-60.

23 [33] Saiwari S, Dierkes W, Noordermeer J. Devulcanization of Whole Passenger Car Tire Material.
24 *KGK Kautschuk, Gummi, Kunststoffe* 2013; 66(7-8 (2013));20-5.

25 [34] Fukahori Y. New progress in the theory and model of carbon black reinforcement of elastomers.
26 *Journal of Applied Polymer Science* 2005; 95(1):60-7.

27 [35] Soares MC, Viana MM, Schaefer ZL, Gangoli VS, Cheng Y, Caliman V, et al. Surface
28 modification of carbon black nanoparticles by dodecylamine: Thermal stability and phase transfer in

1 brine medium. Carbon 2014; 72:287-95.

2 [36] Gómez-Serrano V, Piriz-Almeida F, Durán-Valle CJ, Pastor-Villegas J. Formation of oxygen
3 structures by air activation. A study by FT-IR spectroscopy. Carbon 1999; 37(10):1517-28.

4 [37] Karger-Kocsis J, Mészáros L, Bárány T. Ground tyre rubber (GTR) in thermoplastics,
5 thermosets, and rubbers. Journal of Materials Science 2013; 48(1):1-38.

6 [38] Chen X, Farber M, Gao Y, Kulaots I, Suuberg EM, Hurt RH. Mechanisms of surfactant
7 adsorption on non-polar, air-oxidized and ozone-treated carbon surfaces. Carbon 2003; 41(8):1489-500.

8 [39] Rasines G, Lavela P, Macías C, Zafra MC, Tirado JL, Ania CO. Mesoporous carbon
9 black-aerogel composites with optimized properties for the electro-assisted removal of sodium chloride
10 from brackish water. Journal of Electroanalytical Chemistry 2015; 741:42-50.

11 [40] Liu X, Liu HL, Zhang WX, Li XM, Fang N, Wang XH, et al. Facile synthesis and
12 photocatalytic activity of bi-phase dispersible Cu-ZnO hybrid nanoparticles. Nanoscale Research Letters
13 2015; 10(1):1-9.

14 [41] Darmstadt H, Roy C, Kaliaguine S. Characterization of pyrolytic carbon blacks from
15 commercial tire pyrolysis plants. Carbon 1995; 33(10):1449-55.

16 [42] Majesté J-C, Vincent F. A kinetic model for silica-filled rubber reinforcement. Journal of
17 Rheology (1978-present) 2015; 59(2):405-27.

18 [43] Martínez JD, Puy N, Murillo R, García T, Navarro MV, Mastral AM. Waste tyre pyrolysis - A
19 review. Renewable and Sustainable Energy Reviews 2013; 23:179-213.

20 [44] Senneca O, Salatino P, Chirone R. A fast heating-rate thermogravimetric study of the pyrolysis
21 of scrap tyres. Fuel 1999; 78(13):1575-81.

22 [45] Zhang X, Wang T, Ma L, Chang J. Vacuum pyrolysis of waste tires with basic additives. Waste
23 Management 2008; 28(11):2301-10.

24 [46] Attout A, Yunus S, Bertrand P. Electrospinning and alignment of polyaniline-based nanowires
25 and nanotubes. Polymer Engineering and Science 2008; 48(9):1661-6.

26

27